

of a sex determination gene, *Masculinizer* (responsible for male-specific splicing of *dsx* and repression of transcription from Z chromosomes), has been similarly attributed to misregulation of dosage compensation (33).

Dosage compensation in *A. gambiae* also relies on hyperactivation of the X-chromosome genes in males (34). Therefore, in the presence of YOB, dosage compensation may be directly or indirectly induced in the XX embryos, leading to their death as a result of abnormal overtranscription from both X chromosomes (fig. S10). Conversely, in the absence of YOB, lack of dosage compensation and concomitant insufficient transcription from the X chromosome should be male-lethal, rather than leading to feminization of the XY individuals. Indeed, we observed highly significant male deficiency in mosquitoes surviving transient knockdown of *Yob* in nonsexed embryos (Fig. 3C). All tested female survivors had the XX karyotype.

Involvement of the Y chromosome factor in sex determination in *Anopheles* was first supported by the finding of a single, triploid *Anopheles culicifacies* male with the XXY sex chromosomes (15). Such a karyotype, apparently extremely rare and not reported elsewhere in numerous mutational and cytogenetic studies in *Anopheles*, seems to counter overtranscription of the X-chromosome genes as a cause of female embryo lethality observed in our study. However, the genetic background of this male must have been severely compromised through the mutagenic effects of irradiation on his parents (15). It thus seems likely that the XXY male may have carried multiple mutations, including those causing loss of function of dosage compensation machinery that allowed his survival to adulthood despite possessing two X chromosomes.

A. gambiae and *A. arabiensis* are the most important African vectors of human malaria. Control of the disease depends heavily on the use of insecticides, but emergence of resistance in mosquito populations severely threatens the effectiveness of these approaches (35). The sterile insect technique and other genetic control methods have been proposed to complement current efforts to suppress mosquito populations (36, 37). Such programs must incorporate male-only releases, because released females would contribute to pathogen transmission. However, no effective methods to sex the large number of *Anopheles* needed for releases currently exist. The fitness and mating competitiveness of adults is highly dependent on larval density; therefore, removing females from the release generation during the embryonic stage would drastically decrease the costs of rearing of high-quality males (38). *Yob* represents an excellent tool to be used in transgenic technology to conditionally eliminate female embryos and efficiently produce male-only generations of both malaria-transmitting *Anopheles* species (37).

REFERENCES AND NOTES

- T. Gempe, M. Beye, *BioEssays* **33**, 52–60 (2011).
- A. S. Wilkins, *BioEssays* **17**, 71–77 (1995).
- T. W. Cline, B. J. Meyer, *Annu. Rev. Genet.* **30**, 637–702 (1996).
- J. W. Erickson, J. J. Quintero, *PLOS Biol.* **5**, e332 (2007).
- T. Hiroyoshi, *Genetics* **50**, 373–385 (1964).
- D. Bedo, G. Foster, *Chromosoma* **92**, 344–350 (1985).
- U. Willhöft, G. Franz, *Genetics* **144**, 737–745 (1996).
- J. J. Stuart, G. Mocelin, *Genome* **38**, 673–680 (1995).
- A. Pane, M. Salvemini, P. Delli Bovi, C. Polito, G. Saccone, *Development* **129**, 3715–3725 (2002).
- C. Concha, M. J. Scott, *Genetics* **182**, 785–798 (2009).
- M. Hediger et al., *Genetics* **184**, 155–170 (2010).
- J. N. Shukla, S. R. Palli, *Sci. Rep.* **2**, 602 (2012).
- I. Marin, B. S. Baker, *Science* **281**, 1990–1994 (1998).
- M. J. D. White, *Animal Cytology and Evolution* (Cambridge Univ. Press, Cambridge, ed. 3, 1973).
- R. H. Baker, R. K. Sakai, *J. Hered.* **70**, 345–346 (1979).
- A. B. Hall et al., *Science* **348**, 1268–1270 (2015).
- C. Scali, F. Catteruccia, Q. Li, A. Crisanti, *J. Exp. Biol.* **208**, 3701–3709 (2005).
- Materials and methods are available on *Science Online*.
- J. Kirzynski, D. R. Nusskern, M. K. Kern, N. J. Besansky, *Genetics* **166**, 1291–1302 (2004).
- A. B. Hall et al., *BMC Genomics* **14**, 273 (2013).
- A. B. Hall et al., *Proc. Natl. Acad. Sci. U.S.A.* **113**, E2114–E2123 (2016).
- J. Juhn, A. A. James, *Insect Mol. Biol.* **15**, 363–372 (2006).
- D. Tautz et al., *Nature* **327**, 383–389 (1987).
- D. K. Pritchard, G. Schubiger, *Genes Dev.* **10**, 1131–1142 (1996).
- W. H. Li, in *Molecular Evolution*, W. H. Li, Ed. (Sinauer, Sunderland, MA, 1997), pp. 177–214.
- F. Criscione, Y. Qi, R. Saunders, B. Hall, Z. Tu, *Insect Mol. Biol.* **22**, 433–441 (2013).
- J. C. Lucchesi, T. Skripsky, *Chromosoma* **82**, 217–227 (1981).
- J. P. Gergen, *Genetics* **117**, 477–485 (1987).
- A. Hilfiker, H. Amrein, A. Dübendorfer, R. Schneiter, R. Nöthiger, *Development* **121**, 4017–4026 (1995).
- J. C. Lucchesi, W. G. Kelly, B. Panning, *Annu. Rev. Genet.* **39**, 615–651 (2005).
- M. E. Gelbart, M. I. Kuroda, *Development* **136**, 1399–1410 (2009).
- G. J. Bashaw, B. S. Baker, *Cell* **89**, 789–798 (1997).
- T. Kiuchi et al., *Nature* **509**, 633–636 (2014).
- G. Rose et al., *Genome Biol. Evol.* **8**, 411–425 (2016).
- J. Hemingway et al., *Lancet* **387**, 1785–1788 (2016).
- E. F. Knipling, *Science* **130**, 902–904 (1959).
- L. Alphey, *Annu. Rev. Entomol.* **59**, 205–224 (2014).
- P. A. Papathanos et al., *Malar. J.* **8** (suppl. 2), S5 (2009).

ACKNOWLEDGMENTS

We thank H. Ranson, A. Wilson, and anonymous reviewers for comments and L. Revuelta for technical assistance. This study was supported by funds from the Liverpool School of Tropical Medicine (LSTM), an MRC-LSTM Research Studentship, Wellcome Trust grant 089045/Z/09/Z (J.K. and G.J.L.), and funds from the Pirbright Institute (J.K.). Transgenic mosquitoes used for sexing were developed with Biotechnology and Biological Sciences Research Council grant BB/F021933/1 (G.J.L.). J.K. was partly supported by a subcontract CRSC120816JKUND of the NIH contract HHSN272200900039C. The RNA-seqencing data have been deposited in the Sequence Read Archive repository under the accession numbers SRR953486.1 and SRR953487.1.

SUPPLEMENTARY MATERIALS

www.science.org/content/353/6294/67/suppl/DC1
Materials and Methods
Figs. S1 to S10
Tables S1 to S3
References (39–48)

28 February 2016; accepted 1 June 2016
10.1126/science.aaf5605

CLIMATE CHANGE

Sex-specific responses to climate change in plants alter population sex ratio and performance

William K. Petry,^{1,2*}† Judith D. Soule,² Amy M. Iler,^{2,3} Ana Chicas-Mosier,^{2,4} David W. Inouye,^{2,5} Tom E. X. Miller,⁶ Kailen A. Mooney^{1,2}

Males and females are ecologically distinct in many species, but whether responses to climate change are sex-specific is unknown. We document sex-specific responses to climate change in the plant *Valeriana edulis* (valerian) over four decades and across its 1800-meter elevation range. Increased elevation was associated with increased water availability and female frequency, likely owing to sex-specific water use efficiency and survival. Recent aridification caused male frequency to move upslope at 175 meters per decade, a rate of trait shift outpacing reported species' range shifts by an order of magnitude. This increase in male frequency reduced pollen limitation and increased seedset. Coupled with previous studies reporting sex-specific arthropod communities, these results underscore the importance of ecological differences between the sexes in mediating biological responses to climate change.

Differences between the sexes in morphology and physiology can result in sex-specific responses to the environment (1–3). Given this, climate change may affect the sexes differently, potentially creating an imbalance in the frequency of males and females and altering patterns of fertility and population dynamics (4–6). In so doing, climate change might ameliorate or exacerbate existing sex ratio biases, alternatively driving population growth or decline (4, 7) and affecting the ability of species' ranges to track shifting climate envelopes (8, 9).

We investigated whether climatic variation differentially affects the performance of the sexes

and whether these differences are sufficient to bias population sex ratios. We studied *Valeriana edulis* (valerian, Caprifoliaceae), a dioecious herb with fixed, genetically based sex expression (10, 11), over its entire elevation range from arid low-elevation scrublands to mesic alpine tundra (2000 to 3790 m) and in response to 33 years of climate change. We assessed (i) sex ratio change along these two complementary axes of climate variation, (ii) the sex-specific mechanisms underlying this change, and (iii) how biased sex ratios influence individual fitness.

Climate varies considerably across the elevation range of *V. edulis* (fig. S1, A to D, and

table S2). Contemporary climate data for our study area in the Rocky Mountains of Colorado (fig. S2 and table S1) showed that increasing elevation is accompanied by a decrease in mean growing season (June–August) temperature (-0.59°C per 100 m), an increase in growing season precipitation (1.5 mm per 100 m), a delay in the date of snowmelt (4.1 days later per 100 m), and a marginally significant trend for increasing growing season soil moisture (1.09% per 100 m). Collectively, these changes produce a gradient of decreasing aridity with increasing elevation.

We surveyed population operational sex ratios (OSRs; the proportion of flowering individuals that are male) across this elevation gradient to test whether elevational variation in climate was accompanied by parallel variation in *V. edulis* population OSR. Surveys of 31 *V. edulis* populations across the species' elevation range in 2011 showed that males decrease in frequency with increasing elevation (linear regression, $F_{1,29} = 10.33$, $P = 0.003$, $R^2 = 0.26$) (Fig. 1A), falling from 50.0% of flowering individuals at the lowest elevation population to 22.7% at the highest population, for an average change of -0.88% per 100 m of elevation. Spatial climatic variation thus affects *V. edulis* OSR, suggesting that similar shifts may occur in response to climate change over time.

Recent climate change has warmed and dried our study area, driving climatic isolines up in elevation and providing a temporal axis of cli-

mate variation that parallels that which occurs over the elevation gradient (fig. S1, E to H, and table S2). Data collected during the growing season over the past four decades (1978–2014) show that mean temperature increased $0.21^{\circ}\text{C}/\text{decade}$, precipitation decreased $1.91 \text{ mm}/\text{decade}$, and soil moisture decreased $1.5\%/\text{decade}$, whereas snowmelt date marginally advanced 2.9 days/decade (tables S1 and S2). This change over time is equivalent to an upslope shift in the isolines for growing season mean temperature, precipitation, advancement of snowmelt, and soil moisture at rates of 36 ± 8 , 133 ± 26 , 72 ± 40 , and $195 \pm 523 \text{ m}/\text{decade}$ ($\pm \text{SEM}$), respectively. Climate change over the past four decades has advanced the onset of flowering in *V. edulis* by 3.1 days/decade (linear regression, $P = 0.062$, $R^2 = 0.091$) (fig. S3), likely because of an advancing date of snowmelt, which is strongly associated with flowering phenology in this species (linear regression, $P < 0.0001$, $R^2 = 0.47$) (12). Regional climatic projections suggest that climate will continue to change (13).

Recent climate change has in turn significantly shifted *V. edulis* OSR in a manner consistent with the upslope shift in climate. Surveys of OSR from nine populations in both 1978 and 2011 showed that males have become more frequent across the species' elevation range at a rate of $1.28\%/\text{decade}$ (paired t test, $t_0 = 2.29$, $P = 0.047$) (Fig. 1B). Comparing this temporal shift with the independent, parallel pattern of OSR variation over space shows that OSR isolines are moving upslope at a rate of $175 \text{ m}/\text{decade}$ (lower SE = $87 \text{ m}/\text{decade}$, upper SEM = $316 \text{ m}/\text{decade}$), mirroring the rates at which precipitation and soil moisture have changed. The parallel changes in OSR over elevation and time implicate climate as the driver of OSR variation but do not reveal the processes by which this occurs.

To explore the mechanisms underlying sex-specific responses to climate change, we quantified life history differences between the sexes in four populations spanning 1167 m of elevation (2470 to 3637 m) and varying 22% in

OSR (48 to 26% male). We used sex- and size-structured rates of annual growth and mortality collected from 1978–1980 to calculate male and female life expectancy upon reaching reproductive maturity in each population. This metric integrates sex differences in demographic performance across the life span and reflects the average duration during which a plant contributes to OSR. Sex differences in reproductive life expectancy were concordant with population OSR, so that female-biased OSRs were associated with longer reproductive life spans than those of males (fig. S4) and suggesting that sex-specific effects of climate on life history drive population variation in OSR.

We sought to determine the proximate, physiological basis for the sex-specific effects of climate by focusing on water, a key resource. A plant's water use efficiency (WUE; carbon assimilation per unit of water transpiration) mediates its ability to acquire energy within the short, water-limited growing season (fig. S5). We hypothesized that sex differences in WUE—a trait known to differ between the sexes in many plant species, likely resulting from higher costs of reproduction in females (14)—underlie sex differences in plant performance and drive patterns in OSR. We measured the integrated WUE of each sex as indicated by leaf carbon isotope ratios collected from eight populations varying in OSR (15). Sex differences in WUE strongly predicted population OSR (Deming regression, $t_6 = 2.06$, $P = 0.043$) (Fig. 2); females had higher WUE than that of males in strongly female-biased populations (low OSR), but males had higher WUE than that of females in populations with a higher proportion of males (higher OSR). Although these findings do not directly link WUE to differential performance of the sexes, in other species this trait drives sex differences in performance that produce intrapopulation variation in OSR among arid and mesic microsites (16).

Variation in OSR may feed back to affect population growth by altering pollen availability and seedset rates (7, 17). We measured the response of female seedset to an index of pollen availability

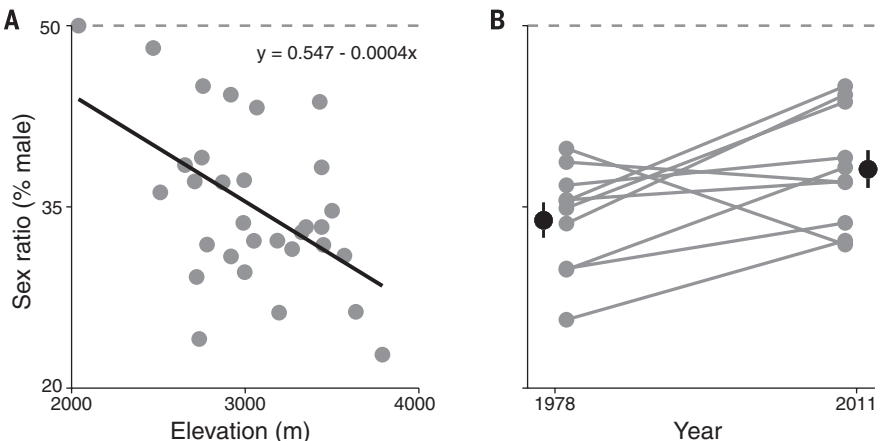


Fig. 1. OSR of *V. edulis* populations declines with climatic variation over elevation and increases in response to climate change. (A) OSR becomes significantly more female-biased with increasing elevation across the species elevation range in contemporary surveys (2011). **(B)** Males have significantly increased in frequency with climate change between 1978 and 2011 by an average of 5.5% ($\pm \text{SEM}$) representing nine resurveyed populations (linked gray time points). A mean of 294 plants were surveyed in each population; populations with <100 flowering plants were censused completely.

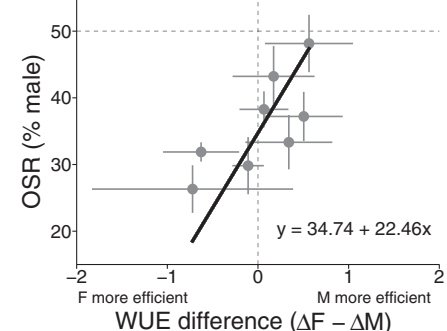


Fig. 2. Sex differences in WUE predict OSR. Each point represents a single population ($n = 8$ populations; 2470 to 3637 m). WUE is inferred from ^{13}C fractionation (Δ), and positive differences between the sexes ($\Delta F - \Delta M$) indicate that WUE of females is lower than that of males and vice versa. Data are means $\pm \text{SEM}$.

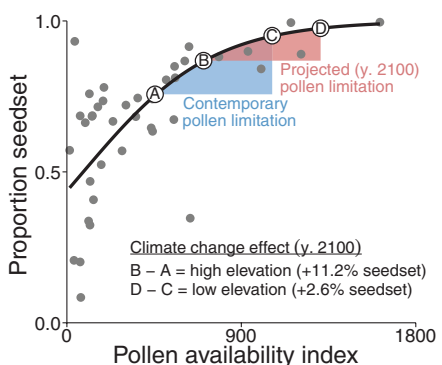


Fig. 3. Pollen availability limits female reproductive success. Each point represents one focal female controlling for competition with neighboring females for pollen. Estimated mean pollen availability for the range of contemporary OSRs observed across the *V. edulis* elevation range and expected OSRs in the year 2100 are indicated by the shaded regions where labeled points ("A" to "D") graphically show the expected change in pollen availability and seedset at the species' range margins. A linear model was fit to logit-transformed data; the back-transformed model fit is shown (12).

within the range of pollen movement (12). The majority (~90%) of pollen was received from males within 10 m of focal females (fig. S6). Female seedset in turn increased with pollen availability in this mating neighborhood (Fig. 3), rising from 39.3 to 99% of flowers producing seed across the observed range of neighborhood pollen availability. Simulating the effect of population OSR on seedset across the range of observed OSRs (Fig. 1A and supplementary materials, materials and methods), we found that the observed spatial variation in OSR was sufficient to alter female fitness. The low frequency of males at high elevation (22.8%) reduced median pollen availability by 55% compared with low-elevation populations with balanced OSR, corresponding to a reduction in seedset from 95 to 76% (Fig. 3). The demographic consequences of these effects are unclear because population growth rate in long-lived species is often relatively insensitive to changes in seed production (18). Nevertheless, *V. edulis* disperses only by seed, and climate effects on seedset may thus have important consequences for range shifts.

A mechanistic understanding of OSR dynamics in this system enables projections of the future state of *V. edulis* populations. Assuming the rate of increase in male frequency continues (1.28%/decade) (Fig. 1B), pollen limitation of reproduction at high-elevation populations could be halved by the year 2100 (a median seedset increase of 11.2%) (Fig. 3), facilitating the upslope range expansion of this species. In contrast, increasing male frequency at low elevation could have little effect on seedset (+2.6%) because females in those populations are pollen-saturated under contemporary, balanced OSRs (Fig. 3). Instead, increasingly male-biased OSRs at low elevation may threaten population viability

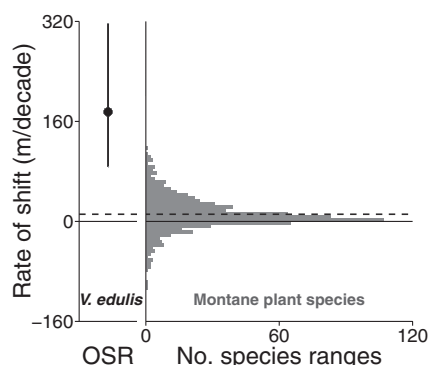


Fig. 4. Elevation range shifts of montane plant species are on average an order of magnitude slower than the rate of *V. edulis* OSR change. (Left) The black point \pm SEM indicates the pace of OSR shift in *V. edulis*. (Right) A histogram shows the observed distribution of range shifts (677 observations encompassing 643 species reported in the literature), and the mean range shift (dashed black line) is indicated.

by replacing females with males and thus reducing population-level seed production (7). Moreover, our previous work shows that female *V. edulis* support dramatically higher densities of arthropods than do males, including several specialist herbivores that depend exclusively on *V. edulis* (19, 20). Accordingly, the effects of a climate-driven decline in female frequency may extend to higher levels of ecological organization.

Our data are distinctive in that they provide a pace of trait change (the upslope shift in plant sex distributions), whereas past studies of distribution responses to climate change have focused on species range shifts. Although trait changes are predicted to occur more rapidly than range shifts (21, 22), the magnitude of such differences is hitherto unknown. Previously reported rates of species range shifts in montane plants show a mean upslope shift of 11.1 m/decade (12), which is dramatically slower than the 175 m/decade upslope pace of OSR change in *V. edulis* (Fig. 4). The pace of species range shifts frequently lags behind the pace of climate change (12), and such range disequilibria are frequently attributed to dispersal limitation (23). In contrast, shifts in traits within species ranges may track climate change more closely because they are based on differential performance of genetically based types that often already exist in many populations across the range. Here, we show that the pace of OSR change in *V. edulis* tracked climate change; it has kept pace with shifts in precipitation and soil moisture and has exceeded those of temperature and snowmelt (fig. S1).

We have demonstrated the occurrence of a potentially widespread form of biological response to climate change. We show that sex specificity of these responses can be exceptionally rapid, with broad effects across multiple scales of ecological organization. Within populations, sex-specific responses to climate change can skew sex ratios—through sex differences in physiology and perfor-

mance or otherwise (5, 9, 24)—and the resulting sex ratio biases may, by mediating reproduction, affect population growth rate, the risk of population extinction, and the rate of adaptation to changing climate by altering the effective population size (25, 26). In so doing, climate-driven changes in sex ratio may also control the tempo of species range shifts by mediating mate limitation at the leading or trailing range margins (8, 9). Accordingly, a full understanding of biological responses to climate change requires a multiscale approach that integrates the underlying, but often cryptic, changes in intraspecific traits that give rise to higher-order patterns.

REFERENCES AND NOTES

- M. A. Geber, T. E. Dawson, L. F. Delph, *Gender and Sexual Dimorphism in Flowering Plants* (Springer, 1999).
- R. Lande, *Evolution* **34**, 292–305 (1980).
- R. Shine, *Q. Rev. Biol.* **64**, 419–461 (1989).
- J.-F. Le Galliard, P. S. Fitz, R. Ferrière, J. Clobert, *Proc. Natl. Acad. Sci. U.S.A.* **102**, 18231–18236 (2005).
- J. M. Calabrese et al., *J. Anim. Ecol.* **77**, 746–756 (2008).
- A. O. Shelton, *Ecology* **89**, 3020–3029 (2008).
- H. Caswell, D. E. Weeks, *Am. Nat.* **128**, 707–735 (1986).
- T. E. X. Miller, B. D. Inouye, *Ecol. Lett.* **16**, 354–361 (2013).
- T. E. X. Miller, A. K. Shaw, B. D. Inouye, M. G. Neubert, *Am. Nat.* **177**, 549–561 (2011).
- O. Meurman, *Soc. Sci. Fennica. Commentationes Biologicae II* **2**, 1–104 (1925).
- J. D. Soule, thesis, Michigan State University, East Lansing (1981).
- Materials and methods are available as supplementary materials on Science Online.
- E. P. Maurer, L. Brekke, T. Pruitt, P. B. Duffy, *Eos Trans. AGU* **88**, 504–504 (2007).
- T. E. Dawson, M. A. Geber, in *Gender and Sexual Dimorphism in Flowering Plants*, M. A. Geber, T. E. Dawson, L. F. Delph, Eds. (Springer, 1999), pp. 175–216.
- G. D. Farquhar, J. R. Ehleringer, K. T. Hubick, *Annu. Rev. Plant Physiol. Plant Mol. Biol.* **40**, 503–537 (1989).
- K. R. Hultine, S. E. Bush, A. G. West, J. R. Ehleringer, *Oecologia* **154**, 85–93 (2007).
- T. M. Knight et al., *Annu. Rev. Ecol. Evol. Syst.* **36**, 467–497 (2005).
- M. Franco, J. Silvertown, *Ecology* **85**, 531–538 (2004).
- W. K. Petry et al., *Ecology* **94**, 2055–2065 (2013).
- K. A. Mooney, A. Fremgen, W. K. Petry, *Arthropod-Plant Interact.* **6**, 553–560 (2012).
- J. Thompson et al., *Proc. Natl. Acad. Sci. U.S.A.* **110**, 2893–2897 (2013).
- J. R. Etterson, R. G. Shaw, *Science* **294**, 151–154 (2001).
- J. P. Sexton, P. J. McIntyre, A. L. Angert, K. J. Rice, *Annu. Rev. Ecol. Evol. Syst.* **40**, 415–436 (2009).
- Y. E. Morbey, R. C. Ydenberg, *Ecol. Lett.* **4**, 663–673 (2001).
- B. Charlesworth, *Nat. Rev. Genet.* **10**, 195–205 (2009).
- D. J. Rankin, H. Kokko, *Oikos* **116**, 335–348 (2007).

ACKNOWLEDGMENTS

We are grateful to the Rocky Mountain Biological Laboratory for facilitating this research over several decades. We are indebted to K. Perry and numerous field and laboratory assistants for data collection and processing; to b. barr, J. Thomson, and J. Harte for snowmelt data; to N. Morueta-Holme for species range data; to T. Huxman for assistance with stable isotope analyses; and to P. CaraDonna for his invaluable comments on a previous draft. Funding sources for this multidecade research are listed in the supplementary materials. Data for this study have been deposited in Dryad (DOI: 10.5061/dryad.lcf8p).

SUPPLEMENTARY MATERIALS

- www.science.org/content/353/6294/69/suppl/DC1
- Materials and Methods
- Supplementary Text
- Figs. S1 to S8
- Tables S1 to S5
- References (27–60)

14 January 2016; accepted 16 May 2016
10.1126/science.aaf2588

Supplementary Material for

Sex-specific responses to climate change in plants alter population sex ratio and performance

William K. Petry,* Judith D. Soule, Amy M. Iler, Ana Chicas-Mosier, David W. Inouye,
Tom E.X. Miller, Kailen A. Mooney

*Corresponding author. Email: william.petry@usys.ethz.ch

Published 1 July 2016, *Science* **353**, 69 (2016)
DOI: 10.1126/science.aaf2588

This PDF file includes:

Materials and Methods
Supplementary Text
Figs. S1 to S8
Tables S1 to S5
Full Reference List

Materials and Methods:

Observed sex ratio assessment and analysis

This study was conducted in Gunnison County and Chaffee County, Colorado USA surrounding the Rocky Mountain Biological Laboratory (RMBL; Fig. S2). Observed population sex ratios of flowering individuals (hereafter OSR) were assessed in fifteen populations (2709-3440m elevation) between 1978 and 1980. Ten populations were relocated and nine were resurveyed in 2011 – the tenth population (Brush Creek Pasture elevation: 2735m) was excluded because the site was both intensely grazed by livestock and regularly hayed. Data for the intervening years between these two time periods were not available, and we accounted for uncertainty of each estimate in our analyses over time. We assessed OSR in these historic populations plus an additional 22 contemporary populations (2040-3790m elevation) in 2011. At each population, we determined the sex of each flowering plant by visual inspection of the flowers until ca. 200 plants were counted along a paced transect or all flowering individuals were censused (range in sampled populations: 197-1284, range in censused populations: 27-172). Sex expression in *V. edulis* is genetically fixed and can only be determined morphologically while flowering. Individuals bearing flowers of both sexes are very rare (<1%), consistent with the rate of sexual inconstancy in other dioecious species (27). Insects are the primary pollinators, typically generalist flies and solitary bees, and *V. edulis* does not reproduce vegetatively. Mature plants flower in >90% of years, and plants may live more than 100 years (11).

We analyzed changes in OSR over elevation and time after logit transformation because OSR is bound by 0 and 1 (i.e. all female and all male, respectively). We calculated the pace of upward OSR shift by estimating the contemporary elevations (Fig. 1A) that correspond to the mean OSRs in 1978 and 2011 (Fig. 1B), then dividing their difference by the intervening 33 years. We report the mean shift after propagating the errors associated with each parameter – the regression slope, the regression intercept, the mean historic OSR, the mean contemporary OSR – using the R package PROPAGATE (28). This package uses a parameter sampling approach and accounts for the covariance structure between parameters; each sample is drawn from a multivariate normal distribution with a covariance matrix constructed from parameter standard deviations. We based all inferences on 10^6 Monte Carlo simulations.

Phenological measurements

The flowering phenology of *V. edulis* has been monitored as part of a community-level flowering phenology survey ca. every 2 d during the growing season (mid April-early October) from 1974-2014 in a series of 2 x 2m permanent plots at the RMBL (29). We recorded the number of stems with open flowers (as opposed to counting all open flowers) of *V. edulis* in each of the 13 plots in which it occurs. There was no census in 1978 or 1990, leaving 39 years of data from 1974-2014.

We analyzed shifts in first, peak, and last flowering dates from the flowering distributions resulting from our surveys. We summed counts of flowering stems across plots in each year to determine the dates of first, peak, and last flowering. First flowering was the first day on which a flowering stem contained flowers in any of the plots, i.e. the very beginning of the across-plot cumulative flowering curve. Peak flowering was

calculated as the day on which 50% of flowering stems were counted (following 30). Last flowering was the last day on which open *V. edulis* flowers were observed. Total flower number was counted instead of the number of flowering stems in six of the 39 years; we removed these years from the analysis of peak flowering date so that all data are consistent across years. The change in measurement unit does not affect the determination of first and last flowering dates.

We regressed each phenological response variable on year to assess shifts in phenology through time. To examine phenological responses to climate, we regressed each response variable on the timing of snowmelt. Timing of snowmelt was the day of first bare ground in a permanent plot at the RMBL (1975-2014; Table S1). We focused on timing of snowmelt as a climatic predictor of flowering phenology following a previous analysis of a subset of our phenology data (30). We also fit a piecewise regression model relating snowmelt to all flowering responses to test for a threshold flowering response to snowmelt (29-31) using the R package SEGMENTED (32). The piecewise model improved the fit for peak flowering date ($\Delta\text{AIC} < 2$) but not first or last flowering date.

First, peak, and last dates of *V. edulis* flowering advanced by 0.60 ± 0.11 , 0.79 ± 0.11 , and 0.63 ± 0.16 days ($\pm \text{SEM}$) for every day that snowmelt advanced, respectively (linear regressions; $P < 0.0005$, $R^2 = 0.47$, $R^2 = 0.62$, $R^2 = 0.30$, respectively). Peak flowering dates did not advance over the earliest range of snowmelt dates on record in the piecewise statistical model ($R^2 = 0.69$). Regardless, the trend towards earlier snowmelt was mirrored by advancing trends in *V. edulis* flowering phenology (linear regressions; first flowering date: -3.1 d/decade, $P = 0.062$, $R^2 = 0.091$; peak: -3.5 d/decade, $P = 0.084$, $R^2 = 0.093$; last: -4.1 d/decade, $P = 0.050$, $R^2 = 0.10$).

Climate data

We assembled climate data across space and time from publicly available databases (33-35) and records shared by colleagues at the RMBL (Table S2, S4). Interpolated and fixed location data were cropped to a $1^\circ \times 1^\circ$ study area centered on the RMBL and enclosing all study populations. Too few weather stations measuring temperature over time, precipitation over time, and soil moisture over space were available within this study area; stations within an expanded $2^\circ \times 2^\circ$ study area were included for these variables. Datasets over time were truncated to years between 1978 and 2014. Elevation data for the study area were acquired from the 30m resolution NASA STRM dataset (36). Changes in climate variables over space and time were assessed with linear regression. Growing season means were determined as the arithmetic mean of monthly means from June-August, inclusive, corresponding to the period between leaf flush and above-ground senescence.

All climate variables were measured or interpolated using standard meteorological sensors with the exception of snowmelt data from personal sensors. Here snowmelt is inferred from HOBO Pendant Temperature/Light data loggers (Onset Computer Corporation, Bourne, Massachusetts) deployed at ground level following Kreuzer et al. (37). Briefly, light reaching the subnivean zone is below the logger detection limit (1 lux between 150-1200 nm) and temperatures remain stable near 0°C . Light infiltration and diurnal fluctuations in temperature were used to mark the melting of snow.

The pace of climate change was calculated for each variable following a similar approach to the calculation of the pace of OSR change (see *Observed sex ratio assessment and analysis*). Briefly, for each climate variable we estimated the expected value at the endpoints of the regression over time (Fig. S1E-H). We then mapped these expected values onto the regressions over space (Fig. S1A-D) to calculate the total elevation displacement over the focal time period (1978-2014). Finally, the pace was calculated by dividing the total displacement by the intervening number of decades (3.6). In parallel with our calculation of the pace of OSR shift, we propagated the errors associated with each regression parameter using 10^6 Monte Carlo simulations in the R package PROPAGATE (28).

Estimation and analysis of historic demographic rates

Sex- and size-specific annual rates of growth and survival were collected in four populations between 1978 and 1980 (11). In each population, >600 individual plants were uniquely tagged. Adult individuals (79-88% of all plants) were binned into 4 size classes (3 in the case of one population, Brush Creek Pasture) by rosette diameter (Table S3). Plants with at least 10 rosette leaves or flowering were considered to be adults. The bounds of the adult size classes were chosen separately for each population using a method that minimizes sampling and distributional errors in the matrix model (38), thus the size classes are not identical among the populations. Sex was determined for all individuals by inspection of the flowers, and those not flowering in any of the 3 years (2-4% of adults) were excluded. Annual rates of growth were calculated as transitions from one size class to another, and shrinkage (i.e. negative growth) was allowed.

For each sex and population combination, annual growth and survival rates were used to populate square transition matrices (39), here restricted to adult stages after the onset of flowering (because pre-reproductive plants could not be sexed). Mean life expectancy for adults at size class 1 was calculated for each matrix following Cochran & Ellner (40) as implemented by the R package IPMPACK v2.1 (41). This quantity measures the remaining life expectancy of plants once they begin flowering and thus reflects the average duration during which a plant contributes to OSR. Relative life expectancy for each population was calculated as the ratio of male to female life expectancy.

Stable isotope analyses

Fully-expanded leaf samples were collected during peak flowering in the summer of 2011, immediately freeze-dried, then stored at -80°C . Samples were prepared for C isotope ratio analysis following Pratt and Mooney (42). Briefly, samples were ground using a Wig-L-Bug bead mill (International Crystal Laboratories, Garfield, NJ) and ca. 1.3 mg of powdered leaf homogenate was packed into 5×9 mm tin capsules. Mass spectrometry was then performed at the University of California, Irvine Stable Isotope Ratio Mass Spectrometry Facility ($\Delta^{13}\text{C}^{\text{plus}}$ XL, Thermo Finnigan, Asheville, NC). Carbon isotope discrimination, $\Delta^{13}\text{C}$, was calculated assuming that $\delta^{13}\text{C}_{\text{air}} = -8.0\text{‰}$ (15). Higher values of $\Delta^{13}\text{C}$ indicate lower WUE. For each population the mean $\Delta^{13}\text{C}$ and the standard error of the mean (SE) were calculated separately for each sex. Relative differences in $\Delta^{13}\text{C}$ between the sexes were calculated by subtracting mean male $\Delta^{13}\text{C}$ from the mean female $\Delta^{13}\text{C}$ and propagating the error. Because both the dependent and independent variables were estimated with error, a generalized Deming regression (R

package DEMING v.1.0-1) that minimized the total sum of squares was used to account for error in both variables (43). Hypothesis tests for Deming regressions use $(n - 2)$ degrees of freedom because means are estimated for both the dependent and independent variables.

Effect of OSR on reproduction

Pollen movement distance was determined by dusting all dehiscent anthers of 12 male *V. edulis* with a fluorescent dye powder (a pollen analogue; 44) at Emerald Lake (3185m) in 2014, then collecting a subsample of flowers from the surrounding female plants along two perpendicular transects centered on the dyed male after 48 hours. All transects were at least 20m long, though females at distances up to 40m were sampled for a subset of 4 of the 12 dyed males. Dye particles were counted only if they were deposited on the stigma, and the distances of these stigmas to the dyed male were recorded. A Lomax (type-II Pareto) distribution was fit to the data to characterize the relationship between distance and dye, yielding parameters scale = 2.20 and shape = 1.24. This distribution predicts that 50% of dye – and by extension pollen – is deposited within 1.65m and 90% is deposited within 11.98m. To maximize replication in a limited space, we assumed a mating neighborhood radius of 10m.

Mating neighborhood (10m radius) composition was measured around 44 randomly chosen focal females at Emerald Lake (14 in 2014 and 30 in 2015 – five focal females in 2015 were later excluded because of heavy ungulate herbivory). A subset of open flowers on each focal female ($\bar{x} = 74$, range: 21-329) was marked on the sepals with a black felt-tip marker, and these flowers were later measured for seed production (0 vs. 1 seed). The distance from the focal female to each plant within the neighborhood was measured to the nearest 5 cm, and all open flowers were counted on each. When the number of flowers was >100 , an estimation technique was used. Briefly, all open flowers were counted in a subset of the inflorescence, then the number of these subsets needed to fill the entire inflorescence was estimated visually. Each observer estimated flowers, then exhaustively counted flowers on a calibration dataset of >20 individuals of each sex. Exploratory analyses revealed differences in estimation among observers, but no observer showed differences in estimations between the sexes. A linear regression relating the estimated number of flowers to the true number of flowers was fit to each observer's calibration dataset. In all cases observer estimations were robust predictors of the true flower number ($0.81 < R^2 < 0.94$; 6 observers). Subsequently all observers used the estimation method and flower estimations were used to estimate the true number of flowers using the parameters of the observer's calibration regression.

Neighborhood composition was determined by measuring: (i) the distance of each neighbor to the focal female, (ii) the total number of plants regardless of sex (= density), and (iii) an index of pollen availability (PC). The PC index assumes that male plant pollen contribution to the focal female increases with the number of male flowers but declines as the distance to the focal female increases (Fig. S6). The PC index was calculated using a modified formula from Garcia-Camacho et al. (45) that allows the decline in male pollen contribution to follow a Lomax distribution:

$$PC_i = \sum_{j=1}^n f_j p(x) d_{ij}$$

where n is the number of males within 10m of the focal female, f_j is the number of open flowers on male j , and $p(x)d_{ij}$ is the probability that pollen is transferred the distance d between focal female i and neighborhood male j given by the Lomax distribution fit to the fluorescent dye dataset.

The proportion of marked flowers on the focal female that set seed was modeled as dependent on neighborhood PC index and female floral density (a surrogate for competition with neighboring females for pollen) after a logit transformation to linearize the response variable (Table S5). Exponential spatial autocorrelation within each year was detected with an effective range of 14m, and this spatial non-independence between neighboring replicates was accounted for in the model using generalized least squares (GLS) regression as implemented in the R package NLME (46, 47).

Simulation of OSR effect on pollen limitation

Detailed mating-scale data from the Emerald Lake population were used to estimate the effect of population-level OSR on mating-scale pollen limitation. Within an arbitrary 200m² of the population, all plants were mapped with a sub-meter accuracy GPS receiver (Trimble GeoXT 6000). The spatial arrangement of plants was modeled as a Thomas cluster point process with an intensity $\lambda = 0.890$, $\kappa = 0.123$, scale = 1.303 using the R package SPATSTAT (48). For the most extreme OSRs observed across the elevation gradient (Fig. 1A), the fitted Thomas point process was simulated 100 times on a 50 × 50m region. Points were randomly assigned a sex based on the OSR and assigned a flower number drawn from the sex-specific distributions of flower number observed at Emerald Lake assuming that flowering frequency is 90%.

To ensure that population-level OSR is indicative of the mean pollination neighborhood composition, the positions of all flowering plants in similar plots were mapped at 3 other populations (collectively spanning 872m elevation and 21% OSR). The spatial arrangement of these plants was treated as a multivariate point pattern consisting of male and female individuals, and the spatial distribution of the sexes was assessed using K functions (49) that test whether one sex is more likely to be surrounded by individuals of the same (positive $K_1 - K_{12}$) or opposite sex (negative $K_1 - K_{12}$). These functions test for aggregation or segregation at multiple spatial scales simultaneously. Under the null hypothesis of random intermixing of the sexes, both K function operations equal zero. Permutations ($n = 1,000$) that randomly assign a sex label to each point were used to construct 95% confidence intervals around the null hypothesis. Significant differences from random intermixing of the sexes occur when the test statistic exceeds the bounds of this interval. This analysis was carried out using the R package ECESPA (50). Although many plant species with separate sexes show spatial segregation of the sexes (51), there was no evidence of spatial aggregation or overdispersion of the sexes relative to one another in any population, demonstrating that population-level OSR reflects the central tendency of the distribution of the sexes at finer scales (Fig. S7).

The effect of distance on pollen availability index (PC) was estimated for each female following the methods described above (see *Effect of OSR on reproduction*). Simulated females less than 10m from the simulated region boundary were excluded to avoid edge effects. The distribution of the pollen availability index (PC) was right skewed, so the median was used to measure central tendency.

Pace of species range shifts

We compiled published reports of species range shifts from large comparative surveys of montane plant distributions over time (52-59). The total elevation displacement (i.e. the change in mean, cover-weighted, or maximum elevation) of each species range was standardized by the time between measurements (3–21 decades). We chose to fit a logistic distribution to the data ($\mu = 10.53$, $s = 14.25$; Fig. S8) because the data showed higher kurtosis than the Normal distribution; the logistic fit was better than the Normal fit ($\Delta AIC = 75.5$). Moreover, this is a conservative choice because the higher kurtosis of the logistic distribution endows it with heavier tails than the Normal distribution.

Previously reported rates of upslope range shift in montane plants ranged from -106.4 to 116.2 m/decade with a mean \pm SEM velocity of 11.5 ± 1.1 m/decade (Fig. 4). Species range shifts of greater or equal magnitude to the pace of *V. edulis* OSR change (175 m/decade) are expected to be exceedingly rare (9.8×10^{-6} ; Fig. S8). Moreover, species range shifts tend to lag behind the pace of climate change (52-54, 56, 57, 60).

Additional author notes:

Sources of funding: WKP was funded by a Graduate Research Fellowship (2010) and Doctoral Dissertation Improvement Grant (DEB 1407318) from the National Science Foundation (NSF). JDS was supported by an NSF Graduate Research Fellowship (1976), a Michigan State University Zoology Department scholarship, and NSF grants DEB 7714811 and DEB 7923945. AMI was funded by a COFUND-Marie Curie Fellowship (2014). Long-term flowering phenology data were supported by NSF grants DEB 7515422, DEB 7807784, BSR 8108387, DEB 9408382, IBN 9814509, DEB 0238331, and DEB 0922080 to DWI and research grants from the University of Maryland's General Research Board and Earthwatch Research Corps also to DWI. ACM was funded by NSF-Research Experience for Undergraduates through DBI 1262713 to the Rocky Mountain Biological Lab (RMBL) and by the Keith Krakauer Scholarship from the RMBL. KAM was supported by NSF grants DEB 1407318 and DEB 1457029.

Author contributions: WKP and KAM developed the overarching study questions. JDS and WKP surveyed 1970's and contemporary population sex ratios, respectively. JDS measured plant demographic rates. AMI and DWI contributed flowering phenology data and analyses. ACM, TEXM, and WKP designed and conducted the study of sex ratio effects on reproduction. WKP analyzed climate, sex ratio, demographic, stable isotope data, and reproductive limitation data. WKP and KAM prepared the manuscript with contributions from all authors.

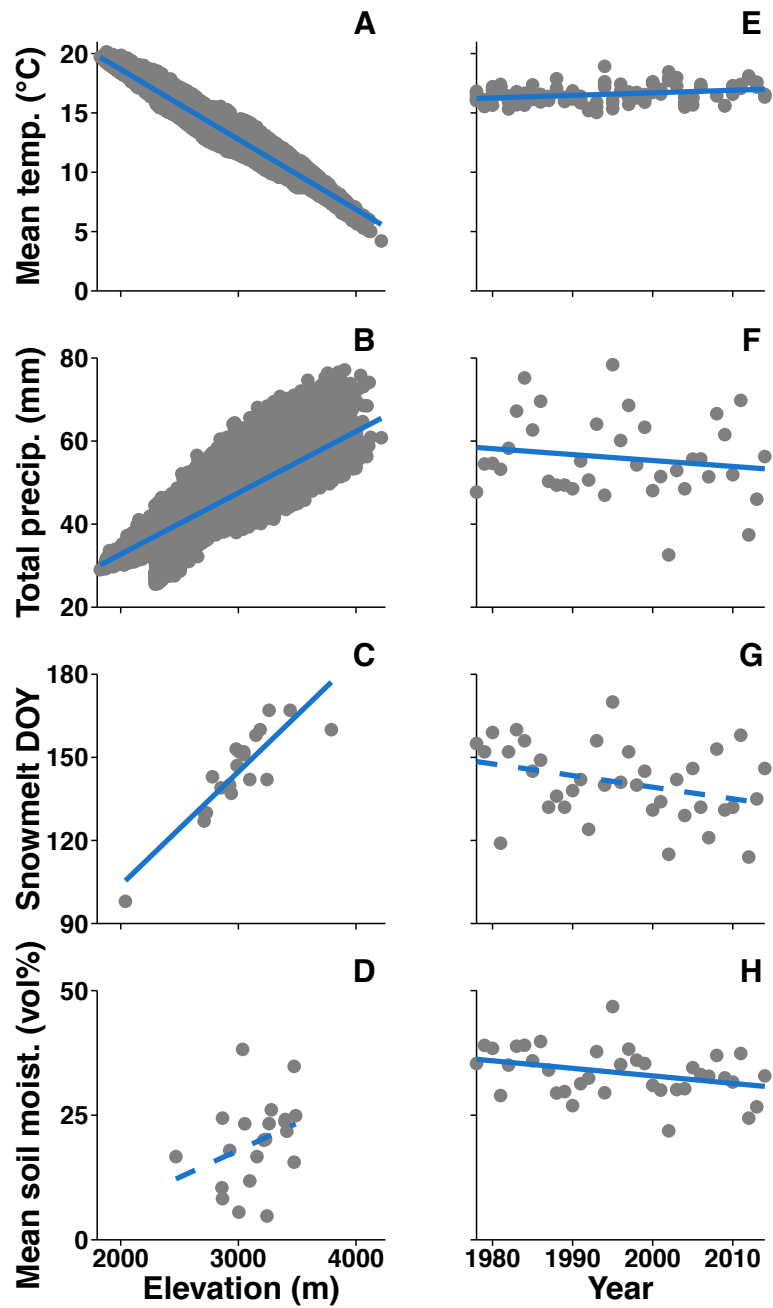


Fig. S1.

Climate changes over space and time in central Colorado, USA. Mean temperature during the growing season (June-August; 1981-2010 normals) declines with elevation (A), and has increased over time (E). Growing season total precipitation increases with elevation (B), but has decreased over time (F). The date of snowmelt delays with elevation (C), and has advanced over time (G). Mean soil moisture during the growing season increases with elevation (D), but decreases over time (H). Solid and dashed lines indicate linear regression slopes that differ from zero ($P < 0.05$) and trends ($P < 0.15$), respectively. See Table S1 for data sources and Table S2 for full summary statistics.

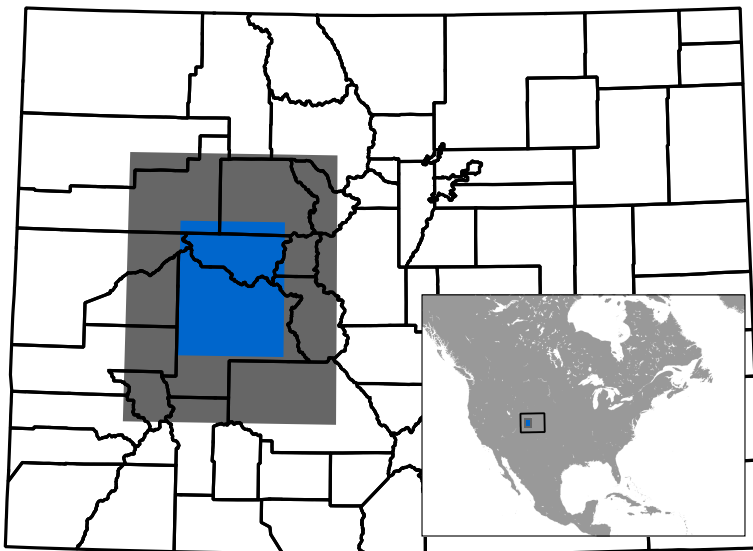


Fig. S2.

Map of study area centered on the Elk and West Elk Mountains of Colorado, USA (inset). Colored shaded regions show the study area (1° in blue and expanded 2° region in gray) in Colorado with county outlines in black.

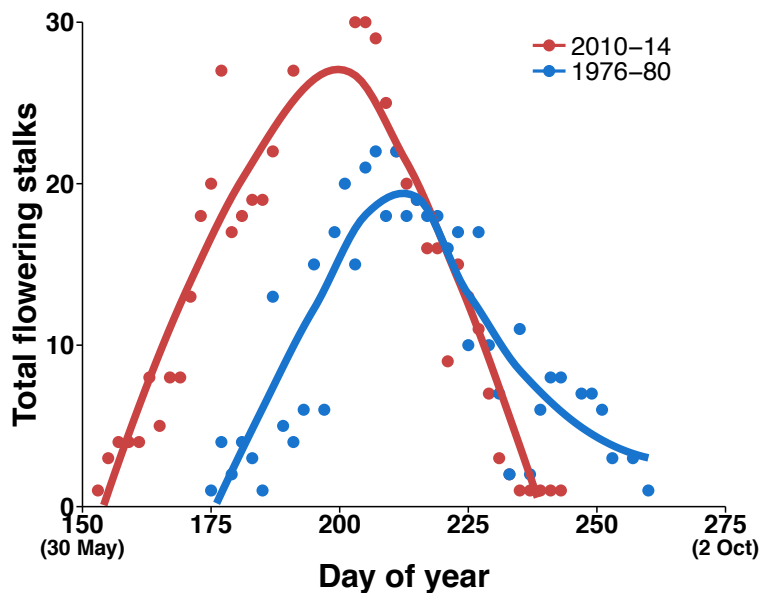


Fig. S3.

The flowering phenology of *Valeriana edulis* has advanced between 1976 and 2014.
Flowering stem counts are summed across all plots in each 5-year window to generate the flowering curve.

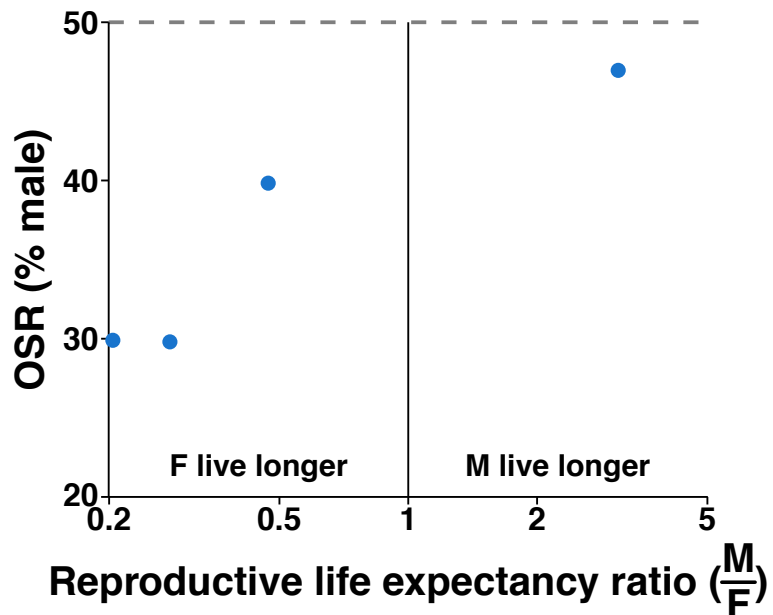


Fig. S4.

Relative life expectancy among the sexes (male/female) at the onset of reproductive maturity corresponds qualitatively to OSR. Note \log_{10} scale of the x-axis that scales deviations in each direction symmetrically about 1. Demographic rates and OSR data were collected between 1978-1980 (see Supplemental Methods and Table S3).

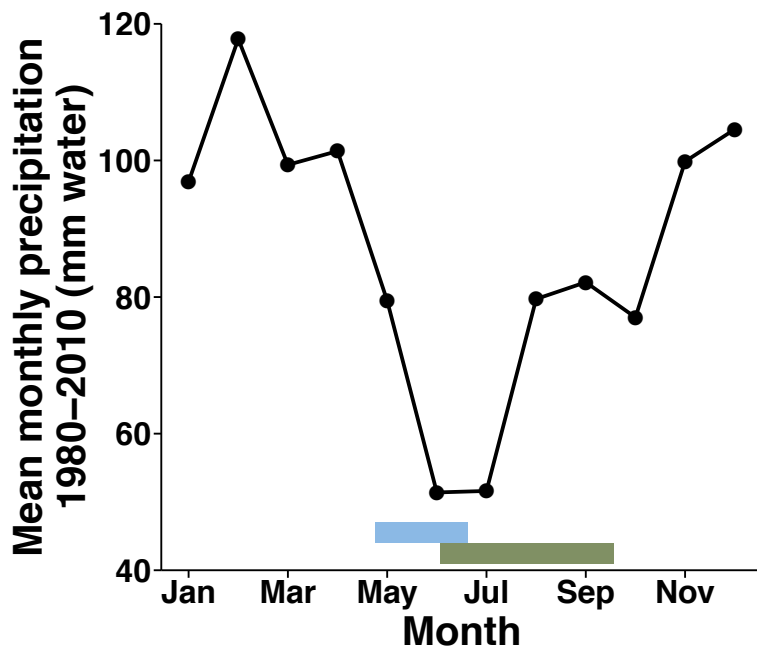


Fig. S5.

The growing season of *V. edulis* occurs during a mid-year dry period. Plants regrow rosettes immediately following snowmelt (1980–2011 range indicated by blue bar) and allocate resources to flowering (1980–2011 range indicated by green bar) prior to the arrival of the late summer monsoon rains. Precipitation data are normals from 1980–2011 from PRISM Climate Group, snowmelt data are from billy barr (see Table S1 for full data source information).

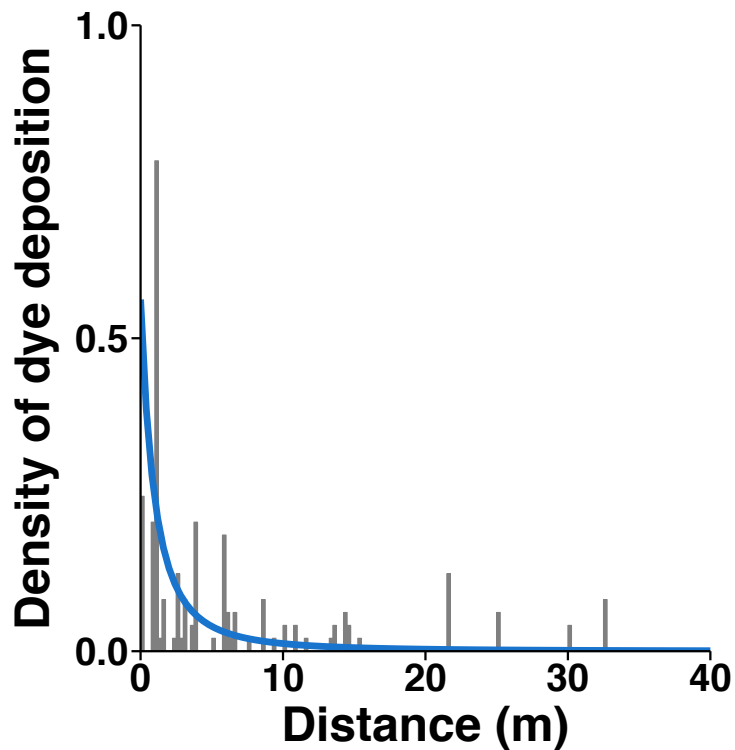


Fig. S6.

Pollen analogue transfer by insect pollinators declines sharply with distance between the pollen donor (male) and the pollen receiver (female). Grey bars indicate the relative frequency of fluorescent dye particle (pollen analogue) transfer from dyed males to neighboring females. The blue line shows a Lomax distribution fit to the data. Pollen analogue deposition decreased sharply with distance, with >95% deposited within 11 m.

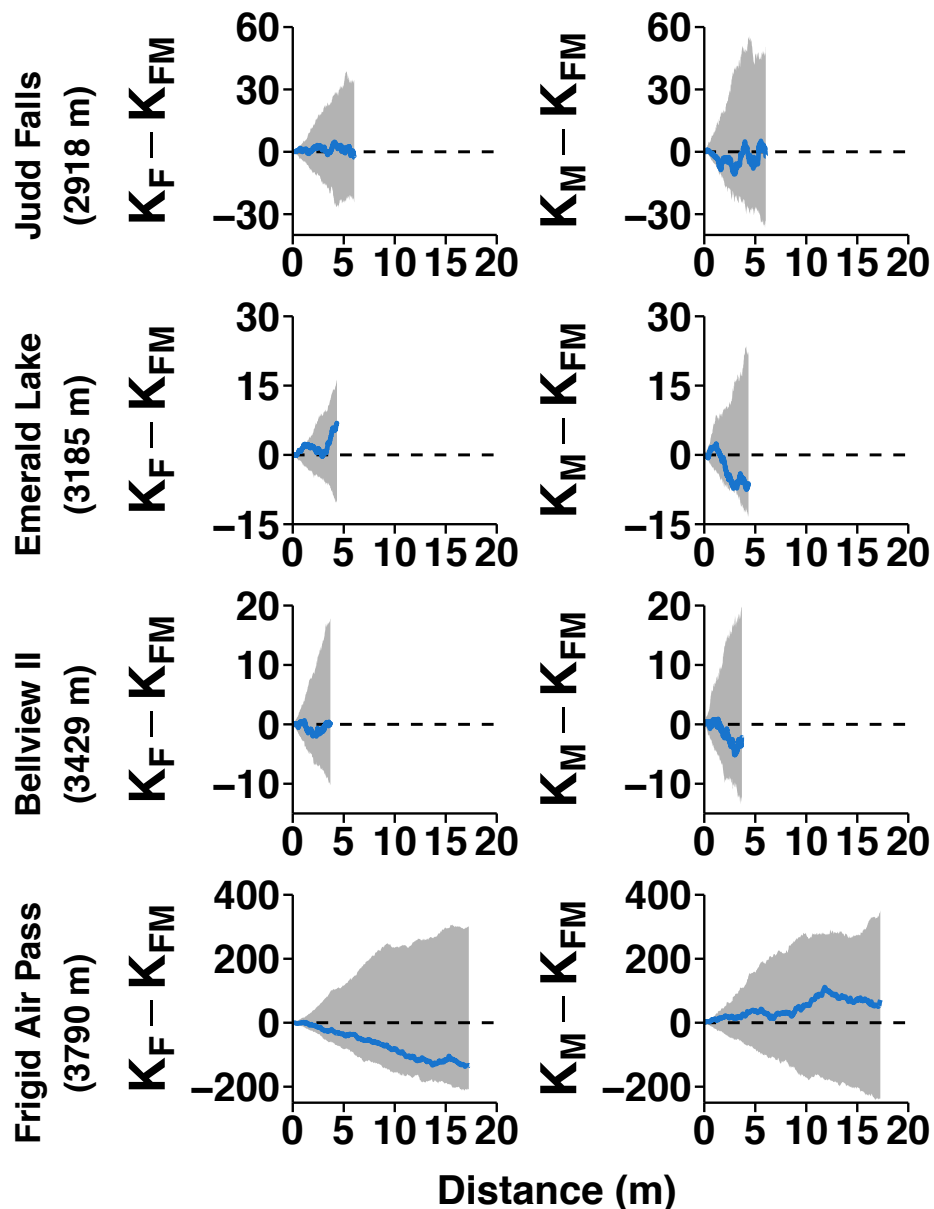


Fig. S7.

Male and female individuals in four populations of *V. edulis* are randomly intermixed in space, showing no evidence of sexual aggregation or segregation across a range of spatial scales. The left column shows tests for females, and the right column shows tests for males. The solid blue line shows the value of the test statistic ($K_x - K_{FM}$, where x is either M for males or F for females); positive values indicate aggregation, and negative values indicate overdispersion. Significant departures from the null hypothesis (0; dashed line) occur when the black line exits the 95% confidence interval around 0 based on 1,000 random permutations (grey shaded region). Differences in the maximum spatial scale of inference are limited by data and spatial constraints of the population.

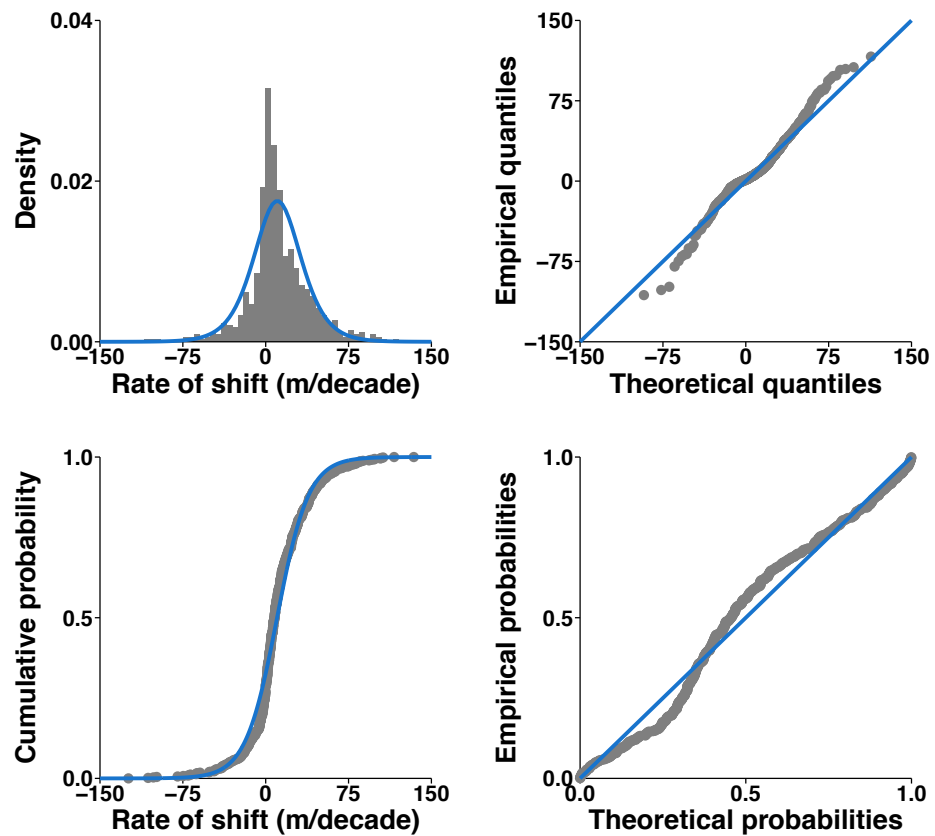


Fig. S8.

Diagnostic plots show a good fit of the logistic distribution to species elevation range shifts. Theoretical values for the probability density function, quantile-quantile plot, cumulative density function, and probability-probability plots are shown as blue lines with empirical data (Fig. 4) shown in grey.

Table S1.

Data sources for climate analyses over space and time. The growing season for *V. edulis* is defined as June (rosette growth initiated) through August (seedset and rosette senescence). Comparisons over time refer to 1978-2014.

Variable	Gradient	Type	Dataset(s)	URL
Growing season mean temperature (°C)	Space	Interpolation	PRISM 1981-2010 Normals (30-arcsecond)	[1]
	Time [†]	Aggregated point sources	NOAA GHCN-M v3	[2]
Growing season precipitation (mm)	Space	Interpolation	PRISM 1981-2010 Normals (30-arcsecond)	[1]
	Time [†]	Aggregated point sources	NOAA GHCN-M v2 SNOTEL	[2] [3]
Snowmelt date (days since 1 Jan.)	Space [†]	Aggregated point sources	SNOTEL, author data loggers, and personal communications (b. barr, D. W. Inouye, J. D. Thompson)	[3,4]
	Time	Single point source	Personal communication (b. barr)	[4]
Soil moisture (vol. %)	Space ^{†‡}	Aggregated point sources	SNOTEL and RMBL weather stations	[3,5]
	Time	Model	NOAA CPC Soil Moisture v2 (0.5 degree)	[6]

[†]Data from 2014 only.

[‡]Study area extended to a 2°×2° around the RMBL because of low station density.

URLs: [1] <http://www.prism.oregonstate.edu>; [2] <http://www.ncdc.noaa.gov/ghcnm/>; [3] <http://www.wcc.nrcs.usda.gov/snow/>; [4] <http://www.gothicwx.org>; [5] <http://www.wrcc.dri.edu/rmbi/>; [6] <http://www.esrl.noaa.gov/psd/>

Table S2.

Summary of linear regressions on climate variable changes over space (elevation in study area) and time (1978–2014). The pace of climate change is the rate of elevational shift in climate isolines over time (see Supplemental Methods), and standard errors of the mean are included in parentheses when appropriate. Data sources for each analysis are listed in Table S1.

Climate variable	Space (100 m^{-1})			Time (decade^{-1})			Pace of climate change (m/decade)
	Slope	R ²	P	Slope	R ²	P	
Growing season mean temperature (°C)	-0.590 (±0.001)	0.94	<0.001	0.215 (±0.059)	0.09*	<0.001	36 (±8)
Growing season precipitation (mm)	1.478 (±0.009)	0.67	<0.001	-1.963 (±0.489)	0.02*	<0.001	133 (±26)
Snowmelt date (days since 1 January)	4.098 (±0.516)	0.77	<0.001	-2.928 (±1.849)	0.06	0.12	72 (±40)
Growing season mean soil moisture (vol%)	1.088 (±0.708)	0.11	0.141	-1.511 (±0.715)	0.11	0.041	195 (±523)

*Partial R² for time when controlling for weather station identity.

Table S3.

Size class bounds for the four historic populations for which demographic data are available (1978-1980). Plant size was measured as the rosette diameter.

Population	Elevation (m)	Adult size 1 (cm)	Adult size 2 (cm)	Adult size 3 (cm)	Adult size 4 (cm)
Brush Creek Pasture	2735	1 – 4	5 – 7	8 – 21	_____
Brush Creek Range	2780	1 – 4	5 – 8	9 – 14	15 – 28
North Rustler's Gulch	2989	1 – 6	7 – 10	11 – 22	23 – 38
Bellview I	3440	1 – 6	7 – 9	10 – 14	15 – 36

Table S4.

Inventory of climate stations used to gather point measurements. Authoritative metadata for each station are available from the data host listed in Table S1. Abbreviations: GHCN = Global Historic Climate Network, SNOTEL = Snow Telemetry, USCRN = United States Climate Reference Network, RMBL = Rocky Mountain Biological Laboratory, T = Temperature, P = Precipitation, Sn = Snowmelt date, So = Soil moisture.

Network(s)	Station name	Station ID	T	P	Sn	So
GHCN	Collbran	42572476007 (v.2)				
		42500051741 (v.3)				
GHCN	Dillon 1E	42572469001 (v.2)				
		42500052281 (v.3)				
GHCN	Gunnison 3SW	42572476002 (v.2)				
		42500053662 (v.3)				
GHCN	Montrose #2	42572476001 (v.2)				
		42500055722 (v.3)				
GHCN	Saguache	42572462008 (v.2)				
		42500057337 (v.3)				
GHCN	Crested Butte	42572476004 (v.3)				
GHCN	Eagle	42574421001 (v.3)				
GHCN	Telluride	42574521006 (v.2)				
SNOTEL	Burro Mountain	378				
SNOTEL	Middle Fork Camp	1014				*
SNOTEL	Summit Ranch	802				
SNOTEL	Copper Mountain	415				
SNOTEL	Fremont Pass	485				
SNOTEL	Hoosier Pass	531				
SNOTEL	Buckskin Joe	938				
SNOTEL	Rough and Tumble	939				
SNOTEL	Brumley	369				
SNOTEL	Park Cone	680				
SNOTEL	Upper Taylor	1141				
SNOTEL	Butte	380				
SNOTEL	Schofield Pass	737				
SNOTEL	Park Reservoir	682				
SNOTEL	Porphyry Creek	701				
SNOTEL	Cochetopa Pass	1059				
SNOTEL	Slumgullion	762				
RMBL	Almont	—				
RMBL	Judd Falls	—				
RMBL	Kettle Ponds	—				
RMBL	Mexican Cut	—				
RMBL	Snodgrass	—				

* Station excluded because of apparent failure of soil moisture sensors at the 20-25 cm depth during the focal time period (i.e. consistently registering 0 despite positive values at other measured soil depths).

Table S5.

Parameter estimates from generalized least squares regression testing for an effect of a pollen availability index on female seed production after logit transformation and controlling for competition with neighboring female flowers for pollen (see Supplemental Methods). Parameters were fit by restricted maximum likelihood (REML) with an exponential spatial correlation structure (range = 15.3m), and all estimates are presented after back-transformation. Both lower and upper standard error estimates (LSE, USE) are reported when they are not approximately symmetric.

Model term	Estimate ± SEM	t	P
Intercept	0.722 ± (0.080, 0.068)	2.570	0.0144
Pollen availability index	0.500 ± 2.19×10^{-4}	3.446	0.0015
Female flower density	-0.501 ± 3.87×10^{-6}	-3.325	0.0020

References and Notes

1. M. A. Geber, T. E. Dawson, L. F. Delph, *Gender and Sexual Dimorphism in Flowering Plants* (Springer, 1999).
2. R. Lande, Sexual dimorphism, sexual selection, and adaptation in polygenic characters. *Evolution* **34**, 292–305 (1980). [doi:10.2307/2407393](https://doi.org/10.2307/2407393)
3. R. Shine, Ecological causes for the evolution of sexual dimorphism: A review of the evidence. *Q. Rev. Biol.* **64**, 419–461 (1989). [Medline doi:10.1086/416458](https://doi.org/10.1086/416458)
4. J.-F. Le Galliard, P. S. Fitze, R. Ferrière, J. Clobert, Sex ratio bias, male aggression, and population collapse in lizards. *Proc. Natl. Acad. Sci. U.S.A.* **102**, 18231–18236 (2005). [Medline doi:10.1073/pnas.0505172102](https://doi.org/10.1073/pnas.0505172102)
5. J. M. Calabrese, L. Ries, S. F. Matter, D. M. Debinski, J. N. Auckland, J. Roland, W. F. Fagan, Reproductive asynchrony in natural butterfly populations and its consequences for female matelessness. *J. Anim. Ecol.* **77**, 746–756 (2008). [Medline doi:10.1111/j.1365-2656.2008.01385.x](https://doi.org/10.1111/j.1365-2656.2008.01385.x)
6. A. O. Shelton, Skewed sex ratios, pollen limitation, and reproductive failure in the dioecious seagrass *Phyllospadix*. *Ecology* **89**, 3020–3029 (2008). [doi:10.1890/07-1835.1](https://doi.org/10.1890/07-1835.1)
7. H. Caswell, D. E. Weeks, Two-sex models: Chaos, extinction, and other dynamic consequences of sex. *Am. Nat.* **128**, 707–735 (1986). [doi:10.1086/284598](https://doi.org/10.1086/284598)
8. T. E. X. Miller, B. D. Inouye, Sex and stochasticity affect range expansion of experimental invasions. *Ecol. Lett.* **16**, 354–361 (2013). [Medline doi:10.1111/ele.12049](https://doi.org/10.1111/ele.12049)
9. T. E. X. Miller, A. K. Shaw, B. D. Inouye, M. G. Neubert, Sex-biased dispersal and the speed of two-sex invasions. *Am. Nat.* **177**, 549–561 (2011). [Medline doi:10.1086/659628](https://doi.org/10.1086/659628)
10. O. Meurman, The chromosome behaviour of some dioecious plants and their relatives with special reference to the sex chromosomes. *Soc. Sci. Fennica. Commentationes Biologicae II* **2**, 1–104 (1925).
11. J. D. Soule, thesis, Michigan State University, East Lansing (1981).
12. Materials and methods are available as supplementary materials on *Science Online*.
13. E. P. Maurer, L. Brekke, T. Pruitt, P. B. Duffy, Fine-resolution climate projections enhance regional climate change impact studies. *Eos Trans. AGU* **88**, 504–504 (2007). [doi:10.1029/2007EO470006](https://doi.org/10.1029/2007EO470006)
14. T. E. Dawson, M. A. Geber, in *Gender and Sexual Dimorphism in Flowering Plants*, M. A. Geber, T. E. Dawson, L. F. Delph, Eds. (Springer, 1999), pp. 175–216.
15. G. D. Farquhar, J. R. Ehleringer, K. T. Hubick, Carbon isotope discrimination and photosynthesis. *Annu. Rev. Plant Physiol. Plant Mol. Biol.* **40**, 503–537 (1989). [doi:10.1146/annurev.pp.40.060189.002443](https://doi.org/10.1146/annurev.pp.40.060189.002443)
16. K. R. Hultine, S. E. Bush, A. G. West, J. R. Ehleringer, Population structure, physiology and ecohydrological impacts of dioecious riparian tree species of western North America. *Oecologia* **154**, 85–93 (2007). [Medline doi:10.1007/s00442-007-0813-0](https://doi.org/10.1007/s00442-007-0813-0)

17. T. M. Knight, J. A. Steets, J. C. Vamosi, S. J. Mazer, M. Burd, D. R. Campbell, M. R. Dudash, M. O. Johnston, R. J. Mitchell, T.-L. Ashman, Pollen limitation of plant reproduction: Pattern and process. *Annu. Rev. Ecol. Evol. Syst.* **36**, 467–497 (2005). [doi:10.1146/annurev.ecolsys.36.102403.115320](https://doi.org/10.1146/annurev.ecolsys.36.102403.115320)
18. M. Franco, J. Silvertown, A comparative demography of plants based upon elasticities of vital rates. *Ecology* **85**, 531–538 (2004). [doi:10.1890/02-0651](https://doi.org/10.1890/02-0651)
19. W. K. Petry, K. I. Perry, A. Fremgen, S. K. Rudeen, M. Lopez, J. Dryburgh, K. A. Mooney, Mechanisms underlying plant sexual dimorphism in multi-trophic arthropod communities. *Ecology* **94**, 2055–2065 (2013). [Medline](#) [doi:10.1890/12-2170.1](https://doi.org/10.1890/12-2170.1)
20. K. A. Mooney, A. Fremgen, W. K. Petry, Plant sex and induced responses independently influence herbivore performance, natural enemies and aphid-tending ants. *Arthropod-Plant Interact.* **6**, 553–560 (2012). [doi:10.1007/s11829-012-9204-5](https://doi.org/10.1007/s11829-012-9204-5)
21. J. Thompson, A. Charpentier, G. Bouquet, F. Charmasson, S. Roset, B. Buatois, P. Vernet, P. H. Gouyon, Evolution of a genetic polymorphism with climate change in a Mediterranean landscape. *Proc. Natl. Acad. Sci. U.S.A.* **110**, 2893–2897 (2013). [Medline](#) [doi:10.1073/pnas.1215833110](https://doi.org/10.1073/pnas.1215833110)
22. J. R. Ettersson, R. G. Shaw, Constraint to adaptive evolution in response to global warming. *Science* **294**, 151–154 (2001). [Medline](#) [doi:10.1126/science.1063656](https://doi.org/10.1126/science.1063656)
23. J. P. Sexton, P. J. McIntyre, A. L. Angert, K. J. Rice, Evolution and ecology of species range limits. *Annu. Rev. Ecol. Evol. Syst.* **40**, 415–436 (2009). [doi:10.1146/annurev.ecolsys.110308.120317](https://doi.org/10.1146/annurev.ecolsys.110308.120317)
24. Y. E. Morbey, R. C. Ydenberg, Protandrous arrival timing to breeding areas: A review. *Ecol. Lett.* **4**, 663–673 (2001). [doi:10.1046/j.1461-0248.2001.00265.x](https://doi.org/10.1046/j.1461-0248.2001.00265.x)
25. B. Charlesworth, Fundamental concepts in genetics: Effective population size and patterns of molecular evolution and variation. *Nat. Rev. Genet.* **10**, 195–205 (2009). [Medline](#) [doi:10.1038/nrg2526](https://doi.org/10.1038/nrg2526)
26. D. J. Rankin, H. Kokko, Do males matter? The role of males in population dynamics. *Oikos* **116**, 335–348 (2007). [doi:10.1111/j.0030-1299.2007.15451.x](https://doi.org/10.1111/j.0030-1299.2007.15451.x)
27. D. Charlesworth, Plant sex determination and sex chromosomes. *Heredity* **88**, 94–101 (2002). [Medline](#) [doi:10.1038/sj.hdy.6800016](https://doi.org/10.1038/sj.hdy.6800016)
28. A.-N. Spiess, propagate: Propagation of uncertainty (2014); available at <http://CRAN.R-project.org/package=propagate>.
29. D. W. Inouye, Effects of climate change on phenology, frost damage, and floral abundance of montane wildflowers. *Ecology* **89**, 353–362 (2008). [Medline](#) [doi:10.1890/06-2128.1](https://doi.org/10.1890/06-2128.1)
30. A. M. Iler, T. T. Høye, D. W. Inouye, N. M. Schmidt, Nonlinear flowering responses to climate: Are species approaching their limits of phenological change? *Phil Trans R Soc B* **368**, 20120489 (2013). [Medline](#) [doi:10.1098/rstb.2012.0489](https://doi.org/10.1098/rstb.2012.0489)
31. H. Steltzer, C. Landry, T. H. Painter, J. Anderson, E. Ayres, Biological consequences of earlier snowmelt from desert dust deposition in alpine landscapes. *Proc. Natl. Acad. Sci. U.S.A.* **106**, 11629–11634 (2009). [Medline](#) [doi:10.1073/pnas.0900758106](https://doi.org/10.1073/pnas.0900758106)

32. V. Muggeo, Segmented: An R package to fit regression models with broken-line relationships. *R News* **8**, 20–25 (2008).
33. PRISM Climate Group, PRISM (2014); available at www.prism.oregonstate.edu.
34. National Operational Hydrologic Remote Sensing Center, Snow Data Assimilation System (SNODAS) Data Products at NSIDC, Version 1. 10.7265/N5TB14TC (2004).
35. Y. Fan, H. van den Dool, Climate Prediction Center global monthly soil moisture data set at 0.5 resolution for 1948 to present. *J. Geophys. Res.* **109** (D10), D10102 (2004). [doi:10.1029/2003JD004345](https://doi.org/10.1029/2003JD004345)
36. T. G. Farr, P. A. Rosen, E. Caro, R. Crippen, R. Duren, S. Hensley, M. Kobrick, M. Paller, E. Rodriguez, L. Roth, D. Seal, S. Shaffer, J. Shimada, J. Umland, M. Werner, M. Oskin, D. Burbank, D. Alsdorf, The shuttle radar topography mission. *Rev. Geophys.* **45**, RG2004 (2007). [doi:10.1029/2005RG000183](https://doi.org/10.1029/2005RG000183)
37. M. Kreuzer Jr., A. M. Ray, R. S. Inouye, H. L. Ray, The use of data loggers to monitor environmental state changes: Snow melt and loss of surface water. *Bull. Ecol. Soc. Am.* **84**, 27–29 (2003). [doi:10.1890/0012-9623\(2003\)84\[27:TUODLT\]2.0.CO;2](https://doi.org/10.1890/0012-9623(2003)84[27:TUODLT]2.0.CO;2)
38. J. Vandermeer, Choosing category size in a stage projection matrix. *Oecologia* **32**, 79–84 (1978). [doi:10.1007/BF00344691](https://doi.org/10.1007/BF00344691)
39. H. Caswell, *Matrix Population Models* (Sinauer Associates, 2001).
40. M. E. Cochran, S. Ellner, Simple methods for calculating age-based life history parameters for stage-structured populations. *Ecol. Monogr.* **62**, 345–364 (1992). [doi:10.2307/2937115](https://doi.org/10.2307/2937115)
41. C. J. E. Metcalf, S. M. McMahon, R. Salguero-Gómez, E. Jongejans, IPMpack: An R package for integral projection models. *Meth. Ecol. Evol.* **4**, 195–200 (2012). [doi:10.1111/2041-210x.12001](https://doi.org/10.1111/2041-210x.12001)
42. J. D. Pratt, K. A. Mooney, Clinal adaptation and adaptive plasticity in *Artemisia californica*: Implications for the response of a foundation species to predicted climate change. *Glob. Change Biol.* **19**, 2454–2466 (2013). [Medline doi:10.1111/gcb.12199](#)
43. T. Therneau, deming: Deming, Thiel-Sen and Passing-Bablock regression (2014); available at <http://CRAN.R-project.org/package=deming>.
44. C. A. Kearns, D. W. Inouye, *Techniques for Pollination Biologists* (Univ. Press of Colorado, 1993).
45. R. García-Camacho, M. Méndez, A. Escudero, Pollination context effects in the high-mountain dimorphic *Armeria caespitosa* (Plumbaginaceae): Neighborhood is something more than density. *Am. J. Bot.* **96**, 1620–1626 (2009). [Medline doi:10.3732/ajb.0800374](#)
46. J. Pinheiro, D. Bates, *Mixed-Effects Models in S and S-PLUS* (Springer Science & Business Media, 2000).
47. J. Pinheiro, D. Bates, S. DebRoy, D. Sarkar, R Core Team, nlme: Linear and nonlinear mixed effects models (2015); available at <http://CRAN.R-project.org/package=nlme>.
48. A. Baddeley, R. Turner, spatstat: An R package for analyzing spatial point patterns. *J. Stat. Softw.* **12**, 1–42 (2005). [doi:10.18637/jss.v012.i06](https://doi.org/10.18637/jss.v012.i06)

49. M. de la Cruz, R. L. Romao, A. Escudero, F. T. Maestre, Where do seedlings go? A spatio-temporal analysis of seedling mortality in a semi-arid gypsophyte. *Ecography* **31**, 720–730 (2008). [doi:10.1111/j.0906-7590.2008.05299.x](https://doi.org/10.1111/j.0906-7590.2008.05299.x)
50. M. de la Cruz, in *Introduccion al Analisis Espacial de Datos en Ecologia y Ciencias Ambientales Metodos y Aplicaciones*, F. T. Maestre, A. Escudero, A. Bonet, Eds. (Madrid, 2008), pp. 76–127.
51. P. Bierzychudek, V. M. Eckhart, Spatial segregation of the sexes of dioecious plants. *Am. Nat.* **132**, 34–43 (1988). [doi:10.1086/284836](https://doi.org/10.1086/284836)
52. A. E. Kelly, M. L. Goulden, Rapid shifts in plant distribution with recent climate change. *Proc. Natl. Acad. Sci. U.S.A.* **105**, 11823–11826 (2008). [Medline](#) [doi:10.1073/pnas.0802891105](https://doi.org/10.1073/pnas.0802891105)
53. G. Parolo, G. Rossi, Upward migration of vascular plants following a climate warming trend in the Alps. *Basic Appl. Ecol.* **9**, 100–107 (2008). [doi:10.1016/j.baee.2007.01.005](https://doi.org/10.1016/j.baee.2007.01.005)
54. A. Bergamini, S. Ungricht, H. Hofmann, An elevational shift of cryophilous bryophytes in the last century – an effect of climate warming? *Divers. Distrib.* **15**, 871–879 (2009). [doi:10.1111/j.1472-4642.2009.00595.x](https://doi.org/10.1111/j.1472-4642.2009.00595.x)
55. J. Lenoir, J. C. Gégout, P. A. Marquet, P. de Ruffray, H. Brisse, A significant upward shift in plant species optimum elevation during the 20th century. *Science* **320**, 1768–1771 (2008). [Medline](#)
56. N. Morueta-Holme, K. Engemann, P. Sandoval-Acuña, J. D. Jonas, R. M. Segnitz, J. C. Svenning, Strong upslope shifts in Chimborazo's vegetation over two centuries since Humboldt. *Proc. Natl. Acad. Sci. U.S.A.* **112**, 12741–12745 (2015). [Medline](#) [doi:10.1073/pnas.1509938112](https://doi.org/10.1073/pnas.1509938112)
57. S. M. Crimmins, S. Z. Dobrowski, J. A. Greenberg, J. T. Abatzoglou, A. R. Mynsberge, Changes in climatic water balance drive downhill shifts in plant species' optimum elevations. *Science* **331**, 324–327 (2011). [Medline](#) [doi:10.1126/science.1199040](https://doi.org/10.1126/science.1199040)
58. Y. Telwala, B. W. Brook, K. Manish, M. K. Pandit, Climate-induced elevational range shifts and increase in plant species richness in a Himalayan biodiversity epicentre. *PLOS ONE* **8**, e57103 (2013). [Medline](#) [doi:10.1371/journal.pone.0057103](https://doi.org/10.1371/journal.pone.0057103)
59. B. Holzinger, K. Hülber, M. Camenisch, G. Grabherr, Changes in plant species richness over the last century in the eastern Swiss Alps: Elevational gradient, bedrock effects and migration rates. *Plant Ecol.* **195**, 179–196 (2008). [doi:10.1007/s11258-007-9314-9](https://doi.org/10.1007/s11258-007-9314-9)
60. I. C. Chen, J. K. Hill, R. Ohlemüller, D. B. Roy, C. D. Thomas, Rapid range shifts of species associated with high levels of climate warming. *Science* **333**, 1024–1026 (2011). [Medline](#) [doi:10.1126/science.1206432](https://doi.org/10.1126/science.1206432)